An Active Contour Model Based on Splines and Separating Forces to Detect the Left Ventricle in Scintigraphic Images

Najah Hraiech[1], Daniel Weinland[2], Kamel Hamrouni[3]
[1] University of Mannheim, Institute for Computer Science V, Mannheim, Germany
hraiech@gmail.com
[2] INRIA: National Institute for Research in Computer Science and Control, Grenoble, France
weinland@inrialpes.fr
[3] ENIT: National Engineering School of Tunis, LSTS Laboratory, Tunis, Tunisia
kamel.hamrouni@enit.rnu.tn

***Abstract*—In this paper we present a novel method for the segmentation of scintigraphic images in order to detect the two ventricles of the heart. The method is based on the active contour model using a region based approach and parametric representation of the contour. The novel aspect of the method is that we have integrated separating forces between the two ventricles in the active contour model. The method has been applied on several scintigraphic images and compared to "active contour without edges" model. The results are satisfactory.**

I. INTRODUCTION

The need in the medical field of knowing how certain organs of the body work, especially to diagnose and determine certain heart diseases, leads to scintigraphy. Scintigraphic imaging techniques can give images of any organ of the body. The organ to be investigated is injected by a radioactive solution. A special camera measures the radiation emitted by a certain organ. One application of these techniques is to capture the geometry of the two heart ventricles.

Usually scintigraphic images are blurred with noise due to artifacts and noise from the gamma camera. As the intensity contrast between the two ventricles and the myocardium is low, the boundaries of the ventricles are often missing in certain locations. Even for skilled personal the exact boundary identification is difficult. Hence segmentation techniques can help us to recognize the two ventricles.

The aim of segmentation is to distinguish objects from background to achieve homogeneous regions. It is widely used for medical image classification.

In this paper we will present a new approach to segment the ventricles based on active contours. While existing active contour approaches can segment the heart in one "homogenous" region, most of them fail in determining the intermediate boundary, which separates the two ventricles.

For the evolution process of two active contours, centered on the right and left ventricle, we demonstrate how by integrating novel separating forces the segmentation can be efficiently improved leading to clearly separated ventricles.

The paper is organized as follows: In the first part, we review the simplified diffusion snake as introduced in [1]. Then we show how to integrate the separating forces. Finally we will give experimental results of our method in separating the two ventricles of the heart, and compare our approach with one of the most widely used active contour approaches, the Chan and Vese model [2].

II. ACTIVE CONTOUR BASED ON SPLINES

The active contour model, or snake, is defined as an energy minimizing functional, where the snake's energy depends on its shape and location within the image. The goal of the active contour is to extract the boundaries of homogeneous regions that constitute an image.

The two most used active contours approaches are: Edge based segmentation approaches [3] and region based segmentation approaches [4, 5, 6]. Edge based active contour approaches are based on gradient information to deform the curve towards the edges of objects within an image. Region based active contours approaches include terms describing the different regions by statistical spatial features, like mean and variance of color values. In our work we use a region based active contour approach, because scintigraphic images are often blurred with noise, and edge based segmentation is known for its sensitivity to noise.

A. Simplified diffusion snake

Our work is derived from the probably most widely studied region based Active Contour approach, which is that of Mumford and Shah [7]. Mumford and Shah proposed to approximate a given input image f with a piecewise smooth function by minimizing the following functional:

$$E(u,C)=\frac{1}{2}\int_{\Omega}(f-u)^2dx+\lambda^2\frac{1}{2}\int_{\Omega-C}|\nabla u|^2dx+\nu|C|, \quad (1)$$

where f is the input image, u is the segmented image, C the segmenting contour, and λ, ν are regularization parameters.

Constraining the segmented image to constant regions, u(x) = u_i, for $x \in R_i$, $R_i \in \Omega$, the Munford-Shah functional (1) simplifies to the cartoon model as:

$$E(u,C) = \frac{1}{2}\sum_i \int_{R_i} (f - u_i)^2 dx + \nu \int_0^1 C_s^2 ds. \quad (2)$$

As representation for the boundary function C we choose a spline representation.

B. Spline representation

The two common ways to represent the contour function are parametric by spline curves, or implicit by the zero level set of a functional: $\Phi \to \Re$, i.e. the intersection of Φ on the zero plane, see [8].

In [2] and [9] T.F. Chan and L.A. Vese explain the implementation of the Mumford-Shah functional using level sets as a representation for the contours.

In our work, we choose a parametric representation based on piecewise polynomial splines. This representation is especially suitable for the integration of the separating forces, which are directly attached onto the control points of the splines.

For the experiments we used the closed, uniform, quadratic and periodic B-spline curve, for more detail see [10] and [11]. Using this spline approximation the contour C has the following form:

$$C : [0,1] \to \Omega, \qquad C(s) = \sum_{n=1}^{N} p_n B_n(s), \quad (3)$$

where B_n are the uniform, periodic, quadratic B-spline basis functions and $p_n = (x_n, y_n)^T$ denote the control points.

C. Curve Evolution

We minimize the energies of the simplified diffusion snake (2), using gradient descent with respect to both, the segmenting contour C and the segmented image u, what leads to the following Euler-Lagrange equation:

$$\frac{dE}{dC} = \left[e^-(s) - e^+(s)\right] \cdot n(s) - \nu C''(s) = 0 \ \forall s \in [0,1], \quad (4)$$

where n is the outer normal vector on the contour for each control point. The terms e^+ and e^- denote the energy density outside and inside the contour C(s) respectively, see [12], defined by:

$$e^{+/-} = (f - u)^2. \quad (5)$$

We solve the minimization problem by gradient descent. The result is summarized in equation (6):

$$\frac{dC(s,t)}{dt} = -\frac{dE(u,C)}{dC} = \left[e^+(s,t) - e^-(s,t)\right] \cdot n(s,t) - \nu C''(s,t) \quad \forall s. \quad (6)$$

In order to obtain an evolution rule for the control points of the spline C we insert the spline curve (3) in equation (6) to derive the following evolution equation for the control points:

$$\sum_{i=1}^{N} \frac{dp_i(t)}{dt} B_i(s) = \left[e^+(s,t) - e^-(s,t)\right] \cdot n(s,t) + \nu \sum_{i=1}^{N} p_i(t) \frac{d^2 B_i(s)}{ds^2}. \quad (7)$$

D. Implementation

Discretizing equation (7) with a set of nodes s_i along the contour gives us a set of linear differential equations. The solution gives the temporal evolution for the coordinates of each control point (x_m, y_m):

$$\frac{dx_m(t)}{dt} = \sum_{i=1}^{N} \left(B^{-1}\right)_{mi} \left[\left(e^+_{s_i} - e^-_{s_i}\right) \cdot n_x + \nu\left(x_{i-1} - 2x_i + x_{i+1}\right)\right], \quad (8)$$

$$\frac{dy_m(t)}{dt} = \sum_{i=1}^{N} \left(B^{-1}\right)_{mi} \left[\left(e^+_{s_i} - e^-_{s_i}\right) \cdot n_y + \nu\left(y_{i-1} - 2y_i + y_{i+1}\right)\right], \quad (9)$$

The matrix B contains the spline basis functions evaluated at the nodes s_i : $B_{i,j} = B_i(s_j)$, (s_i corresponds to the maximum of B_i). Notice, that the matrix B is cyclic and tridiagonal.

The first term in the set of equations (8) and (9) maximizes the homogeneity in the adjoining regions as measured by the energy densities (5). The homogeneity in the adjoining regions forces the contour to recognize the boundaries of the object. The second term smoothes the contour and enforces an equidistant spacing between successive control points.

In our implementation we need at the beginning the initialization of two set of control points (each set corresponds to one ventricle), then we interpolate them by the spline contour. After that, we implement the evolution of this curve as explained in equations (8) and (9).

Note, that with each new iteration, we have first to calculate the new control points (the previous points + the evolution) and then calculate new values for e^+ and e^- depending on the new splines. These two steps are iterated until the difference between the subsequence evolutions is certainly small. For equation (5) we take the difference between inside mean and value of the pixel lying on the inside pointing unit normal of the control; and outside respectively.

E. Discussion

Applying the described actives contours to sample images we realize that the results depend on the initialization: when we have a good initialization the active contour recognizes the two ventricles. With random initialization the results were not

acceptable as the two ventricles are often not separated, illustrated in figure 1 and figure 2.

In the next section we will integrate separating forces in the curve evolution in order to prevent this effect.

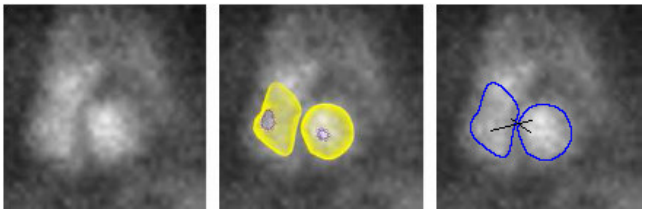

Figure 1. Result of segmentation using Active Contour based on Splines. False initialisation leads to poor final results: (left) original image, (middle) evolution of spline curves, (right) the two curves merge before the splines find the true boundaries.

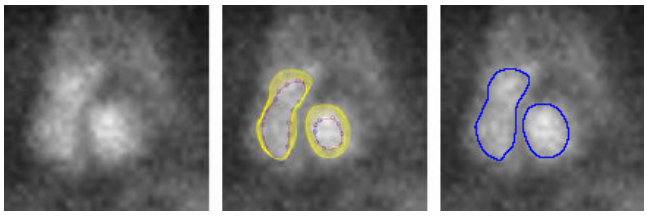

Figure 2. Result of segmentation using Active Contours based on Splines using good initialization: (left) original image, (middle) evolution of spline curves, (right) the segmented images.

III. INTEGRATION OF SEPARATING FORCES BETWEEN THE TWO VENTRICLES

Usually active contours based on splines are a suitable model to recognize boundaries within an image. Nevertheless, using one active contour for every ventricle, experiments showed their tendency to merge ignoring the separating boundary. Therefore, we suggest introducing additional forces into the curve evolution in order to keep the two splines separated from each other.

These forces depend on the distance between the control points on the two contours and are defined as:

$$F_i = \sum_{j=1}^{N} \exp\left(-\left(\frac{\left\| p_i - p_j \right\|_2}{\sigma} \right)^2 \right), \quad (10)$$

so that F_i is the force from all control points j onto the control point i, $i \in C_1$ and $j \in C_2$.

And, vice versa:

$$F_j = \sum_{i=1}^{N} \exp\left(-\left(\frac{\left\| p_j - p_i \right\|_2}{\sigma} \right)^2 \right), \quad (11)$$

so that F_j is the force from all control points i onto the control point j, $i \in C_1$ and $j \in C_2$.

The variance σ controls the region of influence of the forces. Furthermore, $\left\| p_j - p_i \right\|_2$ is the Euclidean distance between two controls points belonging to different curves.

Adding the forces (10) and (11) into equations (8) and (9) leads to the following temporal evolution equation for the coordinates of each control point (x_m, y_m):

$$\frac{dx_m(t)}{dt} = \sum_{i=1}^{N} \left(B^{-1}\right)_{mi} \left[\left(e^+_{s_i} - e^-_{s_i} \right) \cdot n_x + v\left(x_{i-1} - 2x_i + x_{i+1} \right) \right] - h \cdot F_i \cdot n_x, \quad (12)$$

$$\frac{dy_m(t)}{dt} = \sum_{i=1}^{N} \left(B^{-1}\right)_{mi} \left[\left(e^+_{s_i} - e^-_{s_i} \right) \cdot n_y + v\left(y_{i-1} - 2y_i + y_{i+1} \right) \right] - h \cdot F_i \cdot n_y. \quad (13)$$

Regularization parameter h>0 determines the trade-off between the segmenting and the separating forces.

IV. EXPERIENTAL RESULTS

To evaluate our work, we test our implementation with scintigraphic images of different quality. In our implementation we manually initialize the splines. Hereby the number of control points is of importance (see below), while small variations in the initial shape did not affect the results. For the regularization parameters we use an empirical choice.

For most of the images, the tendency of the two splines to merge (figure 1) was successfully suppressed and the evolution of the contours stabilizes around the true boundary of the ventricles (figure 3).

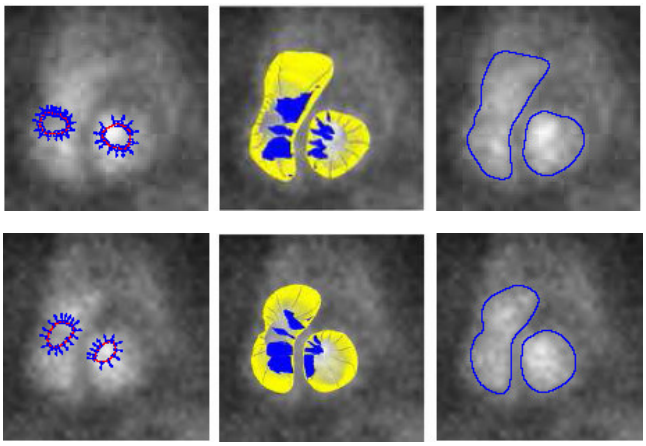

Figure 3. Results using integration of Active Contours based on Splines and forces between the regions of interest: (left) the initialization of spline, (middle) the evolution of spline curves, (right) the segmented images.

Figure 4 shows a comparison of our results with that derived from the Chan and Vese approach [2]. Our method showed to be superior in separating the two ventricles (e.g. figure 4 top row), but has limitations depending on the number of control points (figure 5).

The limitation for the control points is demonstrated as follows: We start from a small contour and the contour grows to

cover the boundaries, but has not a sufficient number of control points to describe the exact shape of the ventricles (figure 5).

For further work we suggest to use a dynamical number of control points, to circumvent the later problem.

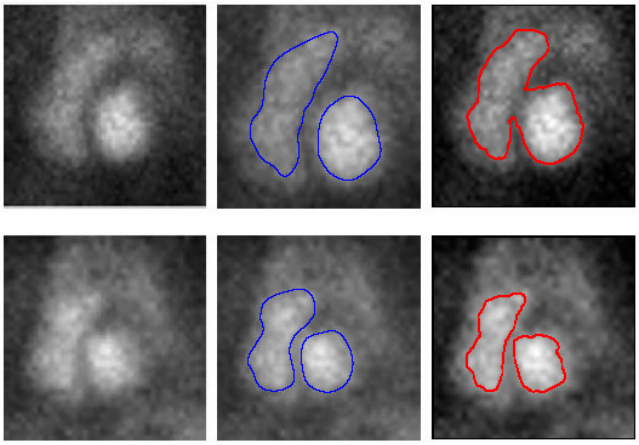

Figure 4. Results of segmentation of the image of the heart: (left) original images, (middle) segmentation with "Integration of separating forces to Active Contours based on Splines", (right) segmentation of original images with "Active Contours Without Edges". (top) the Chan and vese approach fails to separate the two ventrices. (bottom) variations in segmentation dependent on contpour representation (spline vs. level-set)

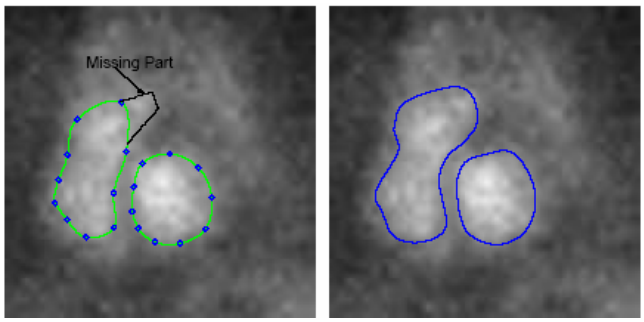

Figure 5. Limitation of controlpoints: (left) the spline describing the boundary has not enough control points to cover the whole region, (right) true segmentation result derived with sufficient control points.

V. CONCLUSION

In this paper, we proposed a new active contour method using a uniform quadratic B-spline linked with extra forces to implement a region-based active contour segmentation algorithm for scintigraphic images.

We conclude that the integration of separating forces into active contours model improves the segmentation of the two ventricles, compared to common active contour approaches.

To show the performance of our results, we compared it with the "Active Contour without edges" approach [2].

ACKNOWLEDGMENT

This work was partially done while visiting the CVGPR group, University of Mannheim, Germany.

REFERENCES

[1] Daniel Cremers, Christoph Schnoerr, and Joachim Weickert. "Diffusion-snakes: Combining Statistical Shape Knowledge and Image Information in a Variational Framework". IEEE Workshop on Variational and Level Set Methods, Vancouver, CA, July. 13, 2001, pp. 137-144 IEEE.

[2] Tony F. Chan and Luminita A. Vese. "Active Contours Without Edges". IEEE Transactions on image processing, Vol.10, No. 2, February 2001.

[3] M. Kass, A. Witkin, and D. Terzopoulos. "Snakes: Active contours models". International Journal of Computer Vision, pages 321–331, 1988.

[4] S. Zhu and A. Yuille, "Region competition: unifying snakes, region growing, and bayes/MDL for multiband image segmentation," PAMI, vol. 18, pp. 884–900, september 1996.

[5] N. Paragios and R. Deriche, "Geodesic active regions: A new paradigm to deal with frame partition problems in computer vision," JVCIR, vol. 13, pp. 249–268, 2002.

[6] Ronfard R. "Region-based strategies for active contour models" International Journal of Computer Vision, Vol. 13, No. 2, pp. 229-251, Oct. 1994.

[7] D. Mumford and J. Shah. "Boundary detection by minimizing functionals". In Proc. IEEE Conf. Computer Vision and Pattern Recognition, 1985.

[8] J.A.Sethian, "Level Set Methods", Cambridge University Press, 1996.

[9] Tony F. Chan and Luminita A. Vese. "A Level Set Algorithm for Minimizing the Mumford-Shah functional in image processing". In IEEE Workshop on Variational and Level Set Methods (VLSM'01), Vancouver, Canada, July 2001.

[10] Gerald Farin, "Curves and Surfaces for Computer-Aided Geometric Design". Academic Press, San Diego, 1997.

[11] R. H. Bartels, J. C. Beatty, and B. A. Barsky, "An introduction to Splines for use in Computer Graphics and Geometric Modeling", Morgan-Kaufmann, Los Altos, Californie, 1987.

[12] D. Mumford and J. Shah. Optimal approximations by piecewise smooth functions and associated variational problems. Comm. Pure Appl. Math., 42:577-685, 1989.